Organic & Biomolecular Chemistry

PAPER

Cite this: *Org. Biomol. Chem.*, 2017, **15**, 1828

Stereoisomers of oseltamivir – synthesis, *in silico* prediction and biological evaluation†

Viktória Hajzer,[a] Roman Fišera,*[a] Attila Latika,[a] Július Durmis,[a] Jakub Kollár,[b,c] Vladimír Frecer,[d,e] Zuzana Tučeková,[f] Stanislav Miertuš,[e,f] František Kostolanský,[g] Eva Varečková[g] and Radovan Šebesta*[h]

Received 6th December 2016,
Accepted 26th January 2017

DOI: 10.1039/c6ob02673g

rsc.li/obc

Oseltamivir is an important antiviral drug, which possess three chirality centers in its structure. From eight possible stereoisomers, only two have been synthesized and evaluated so far. We describe herein the stereoselective synthesis, computational activity prediction and biological testing of another three diastereoisomers of oseltamivir. These isomers have been synthesized using stereoselective organocatalytic Michael addition, cyclization and reduction. Their binding to viral neuraminidase N1 of influenza A virus was evaluated by quantum-chemical calculations and their anti-influenza activities were tested by an *in vitro* virus-inhibition assay. All three isomers displayed antiviral activity lower than that of oseltamivir, however, one of the stereoisomers, (3*S*,4*R*,5*S*)-isomer, of oseltamivir showed *in vitro* potency towards the Tamiflu-sensitive influenza viral strain A/Perth/265/2009(H5N1) comparable to Tamiflu.

Introduction

Influenza is one of the most common and dangerous viral respiratory diseases. According to the World Health Organization (WHO), seasonal influenza epidemics are responsible for up to 500 000 deaths each year.[1]

Oseltamivir phosphate (Tamiflu) is one of the most effective antiviral drugs currently available on the market. It is included on the WHO's list of essential medicines,[2] and was FDA approved for the treatment and prophylaxis of severe or complicated infections due to influenza A and B viruses. Oseltamivir phosphate is a pro-drug of the active metabolite, oseltamivir carboxylate, which is a selective inhibitor of viral neuraminidase enzymes of the influenza virus. Neuraminidases that exist in a variety of subtypes named N1–N9 are glycoproteins located on the surface of influenza virions and are essential for the release and spread of newly formed viral particles from the infected host cells.[3] Due to the fear of potential pandemic flu outbreak, there has been great interest from both academic and industrial laboratories in the syntheses of oseltamivir. Currently, oseltamivir is manufactured by Roche starting from shikimic acid.[4] Apart from this procedure, however, there was a large array of diverse syntheses developed.[5] Due to their efficiency and user friendliness, organocatalytic procedures are particularly appealing. Enders' discovery that prolinol silyl ether can assemble a cyclohexene core in one reaction step from an enal, nitroalkene and aldehyde, served as inspiration for the development of organocatalytic syntheses of oseltamivir.[6] Based on this precedent, Hayashi has developed a short synthesis of oseltamivir using prolinol silyl ether-catalyzed Michael addition to nitroacrylate as a key step.[7] This methodology necessitated the transformation of the ester group into the amino group *via* the potentially hazardous Curtius rearrangement. To circumvent this issue, the use of a Michael acceptor, which already contains an acetamido group has been proposed.[8] Further improvements have recently been suggested by Hayashi.[9] Our laboratory also investigated the possibilities of using acetals as a starting material in the Michael addition.[10] Organocatalytic Diels–Alder reactions can also serve as a basis for oseltamivir synthesis.[11]

Drug resistance of influenza viruses is becoming a serious problem, therefore, syntheses of new antiviral medicines

[a]*SYNKOLA, Ltd, Mlynská dolina, Ilkovičova 6, SK-84215 Bratislava, Slovakia. E-mail: fisera@synkola.sk*
[b]*Comenius University in Bratislava, Faculty of Pharmacy, Department of Pharmaceutical Analysis and Nuclear Pharmacy, Odbojárov 10, SK-83232 Bratislava, Slovakia*
[c]*Comenius University in Bratislava, Faculty of Mathematics, Physics and Informatics, Department of Nuclear Physics and Biophysics, Mlynská dolina, SK-84248 Bratislava, Slovakia*
[d]*Comenius University in Bratislava, Faculty of Pharmacy, Department of Physical Chemistry of Drugs, Odbojárov 10, SK-83232 Bratislava, Slovakia*
[e]*ICARST n.o., Jamnického 19, SK-84104 Bratislava, Slovakia*
[f]*University of SS. Cyril and Methodius, Faculty of Natural Sciences, Department of Biotechnologies, Námestie J. Herdu 2, SK-91701 Trnava, Slovakia*
[g]*Biomedical Research Center, Institute of Virology, Slovak Academy of Sciences, Department of Orthomyxovirus Research, Dúbravská cesta 9, SK-84505 Bratislava, Slovakia*
[h]*Comenius University in Bratislava, Faculty of Natural Sciences, Department of Organic Chemistry, Mlynská dolina, Ilkovičova 6, SK-84215 Bratislava, Slovakia. E-mail: radovan.sebesta@fns.uniba.sk*

† Electronic supplementary information (ESI) available: Pictures of NMR spectra. See DOI: 10.1039/c6ob02673g

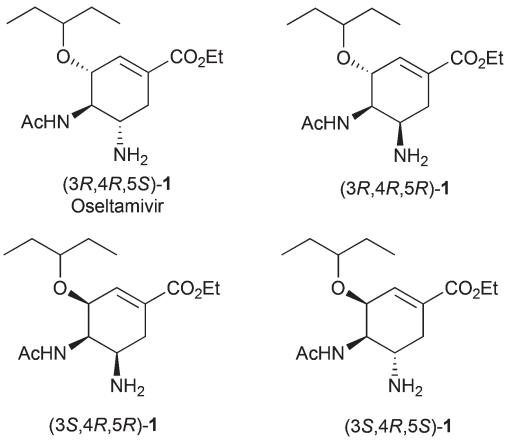

Fig. 1 Chemical structures of synthesized stereoisomers of oseltamivir.

remain an important goal of the medicinal chemistry research. Oseltamivir contains three stereogenic centers and thus it can exist in the form of eight stereoisomers. Oseltamivir phosphate itself has a (3*R*,4*R*,5*S*) configuration. Another stereoisomer of oseltamivir has been synthesized and its properties were investigated by Sartori, Zanardi and coworkers.[12] Other stereoisomers of oseltamivir have not been described so far. There is a possibility that different stereoisomers of oseltamivir will give rise to altered interactions with the chiral environment of its biological target, the viral neuraminidase, and thus display different, hopefully improved, antiviral activities. In this context, we decided to synthesize three, so far untested, stereoisomers of oseltamivir, to predict their inhibitory activities through molecular modeling and evaluate their antiviral efficiency using *in vitro* biological testing (Fig. 1).

Results and discussion

Synthesis

Starting materials for the syntheses of oseltamivir isomers are not commercially available and were prepared according to previously described procedures. Aldehyde **2** was synthesized by nucleophilic epoxide opening of oxiran-2-ylmethanol with pentan-3-ol followed by a periodate cleavage of the intermediary diol (Scheme 1a).[8b] Nitroalkene **3** was synthesized from nitromethane, *N*-methylaniline and triethylorthoformate (Scheme 1b).[13] Phosphonate **4** was synthesized by an aldol condensation of ethyl 2-(diethoxyphosphoryl)acetate with formaldehyde (Scheme 1c).[14]

The first step in the organocatalytic synthesis of oseltamivir and its stereoisomers is a Michael addition. The reaction was performed with aldehyde **2** and nitroalkene **3** in the presence of mandelic acid as an acidic additive and a Jørgensen–Hayashi catalyst ((*S*)-**C1**). The corresponding Michael adducts **5** were isolated as a mixture of *syn* and *anti*-diastereomers (Scheme 2). The diastereomers were then separated by flash chromatography. Both diastereomers were obtained in high enantiomeric purity, er 97 : 3 and 98 : 2 respectively.

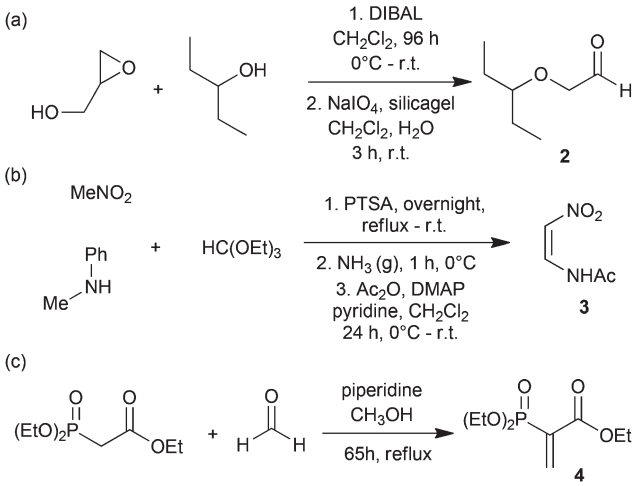

Scheme 1

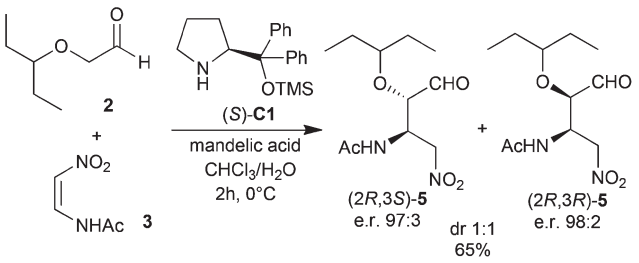

Scheme 2

The Michael adduct (2*R*,3*S*)-**5** and phosphonate **4** were assembled into a cyclohexene derivative **6** *via* a combination of another Michael addition and Horner–Wadsworth–Emmons reaction (Scheme 3). The cyclohexene derivative **6** was obtained as a mixture of two diastereomers with dr 2 : 1 (5*R*/5*S*). These diastereoisomers were again separated by flash chromatography.

Reduction of the nitro group by zinc in aqueous acetic acid yielded oseltamivir (**1**). Starting from the isomer (3*R*,4*R*,5*S*)-**6**, oseltamivir itself (3*R*,4*R*,5*S*)-**1** was synthesized.

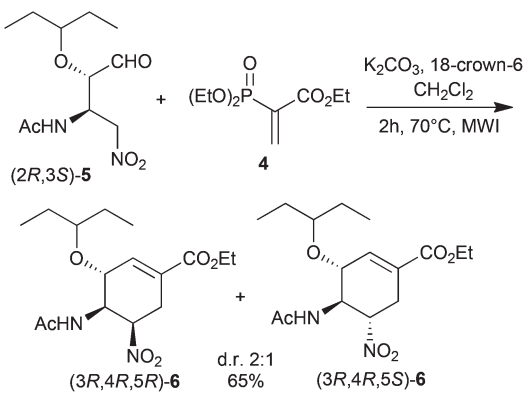

Scheme 3

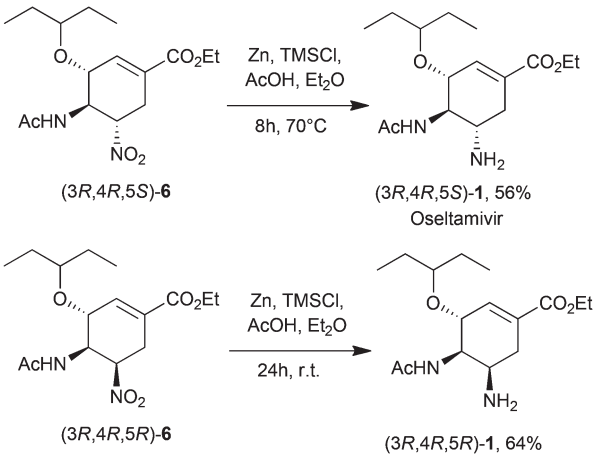

Scheme 4

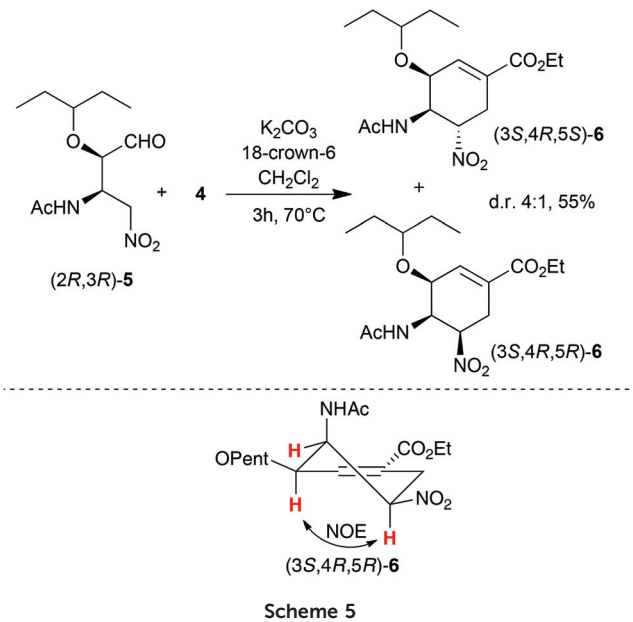

Scheme 5

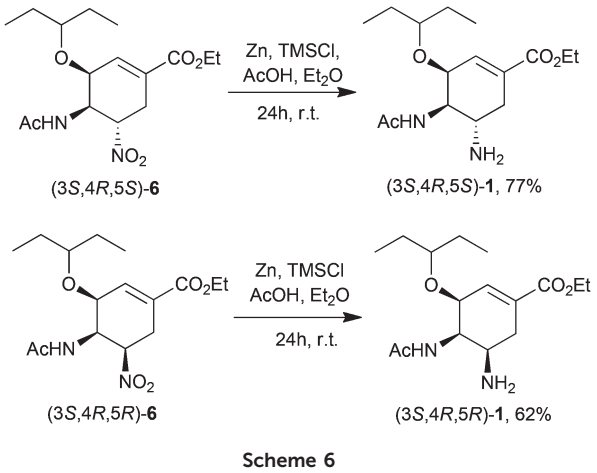

Scheme 6

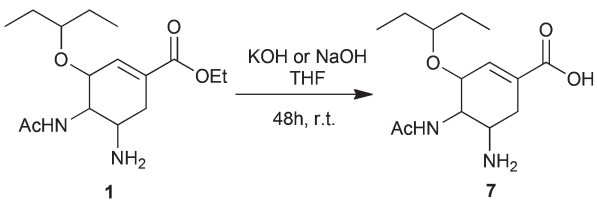

Scheme 7

Starting from an (*R*,*R*)-diastereomer of the Michael adduct **5**, cyclization with phosphonate **4** provided another two diastereoisomers of cyclohexene derivative **6** (Scheme 5). The cyclization of (*R*,*R*)-**5** provided derivative **6** with a higher diastereomeric ratio dr of 4 : 1 (5*S*/5*R*) than the corresponding reaction of (*R*,*S*)-**5**. The diastereoisomers were separated by flash chromatography. Enantiomeric purities of these isomers were slightly lower; er 74 : 26 (3*S*,4*R*,5*S*)-**6** and er 90 : 10 for the (3*S*,4*R*,5*R*)-**6** isomer. Lowering of the enantiomeric purity of compounds **6** could have been caused by a non-catalysed partial retro-Michael reaction during the cyclization process. A relative configuration at the C-5 carbon has been determined by qDQCOSY and NOESY spectroscopy. An important NOE crosspeak between H-3 and H-5 hydrogens, which has been observed, can be possible only in the (3*S*,4*R*,5*R*)-**6** derivative (Scheme 5).

Similar to previous isomers, reduction of the nitro group was performed by zinc in acetic acid. In this way, reduction of cyclohexene derivatives (3*S*,4*R*,5*S*) and (3*S*,4*R*,5*R*)-**6** afforded the corresponding oseltamivir diastereomers (3*S*,4*R*,5*S*) and (3*S*,4*R*,5*R*)-**1** (Scheme 6). Relative configurations of amines **1** were determined by NOESY and qDQCOSY spectra. A NOE crosspeak between H-3 and H-5 was observed in (3*S*,4*R*,5*R*)-**1**, similar to derivatives (3*S*,4*R*,5*R*)-**6**.

Oseltamivir is actually a pro-drug, which is hydrolyzed in acidic media in the stomach. Therefore, for biological testing, all oseltamivir isomers **1** were hydrolyzed under basic conditions to the corresponding carboxylic acids **7** (Scheme 7).

The synthesis of the remaining undescribed oseltamivir stereoisomers would be possible by the application of the opposite enantiomer of the Jørgensen–Hayashi catalyst (*R*)-**C1** in the Michael addition (Scheme 2). From the corresponding Michael adducts and by following cyclization and reduction steps (Scheme 3 and 4), it should be possible to prepare the remaining undescribed oseltamivir stereoisomers.

Molecular modelling

Molecular modelling and computational prediction of stability of stereoisomers of the active metabolite of oseltamivir in aqueous solution (zwitterionic oseltamivir carboxylate (**7**), Fig. 2) were carried out by means of density functional theory (DFT). Calculations suggested a relative stability of the eight possible stereoisomers as shown in Table 1.[15]

In the most stable enantiomers V, (3*S*,4*R*,5*R*)-**7**, and VI, (3*R*,4*S*,5*S*)-**7**, of the oseltamivir carboxylate the cyclohexene ring forms two half-chair conformations $^{5}H_{4}$ and $^{4}H_{5}$ with both the 3-oxypentyl group and the 5-amino group oriented to

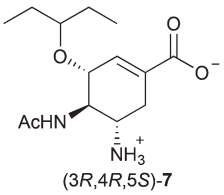

(3*R*,4*R*,5*S*)-**7**

Fig. 2 Zwitterionic form of hydrolyzed oseltamivir at neutral pH.

Table 1 Predicted relative stabilities $\Delta\Delta E_{tot,sol}$ of stereoisomers of oseltamivir carboxylate in water

Stereoisomer[a]	$\Delta\Delta E_{tot,sol}$ [b] [kcal mol^{-1}]	Cyclohexene ring puckering[c]
I. (3*R*,4*R*,5*S*)-**7**[d]	0.0	$^5H_4$
II. (3*S*,4*S*,5*R*)-7	0.0	$^4H_5$
III. (3*S*,4*R*,5*S*)-7	−1.5	$^5H_4$
IV. (3*R*,4*S*,5*R*)-7	−1.5	$^4H_5$
V. (3*S*,4*R*,5*R*)-7	−1.8	$^5H_4$
VI. (3*R*,4*S*,5*S*)-7	−1.8	$^4H_5$
VII. (3*S*,4*S*,5*S*)-7	−0.8	$^4H_5$
VIII. (3*R*,4*R*,5*R*)-7	−0.8	$^5H_4$

[a] 3 chiral centers = 4 diastereoisomers of 2 enantiomers each, Fig. 3. [b] $\Delta\Delta E_{tot,sol}$ – relative difference in total energies of solvated stereoisomers computed for optimized molecular geometries (zwitterions of a total charge q = 0, Fig. 2) by DFT method (DFT-B3LYP-SCRF/6-31+G*) using Gaussian 09.[18] Stereoisomer I. (3*R*,4*R*,5*S*)-oseltamivir carboxylate was taken as the reference structure. Higher value of $\Delta\Delta E_{tot,sol}$ means lower stability of the pertinent stereoisomer. [c] Cyclohexene ring puckering in the notation of Sartori *et al.*[12] The conformer $^4H_5$ has its carbon C4 placed above the plane defined by the ring double bond and the carboxylic group C2═(C1–COO–)–C6 (Fig. 3 and 4) while carbon C5 is positioned below this plane. [d] Configuration of stereoisomer I. (3*R*,4*R*,5*S*)-7 (oseltamivir) carboxylate corresponds to that of Tamiflu.

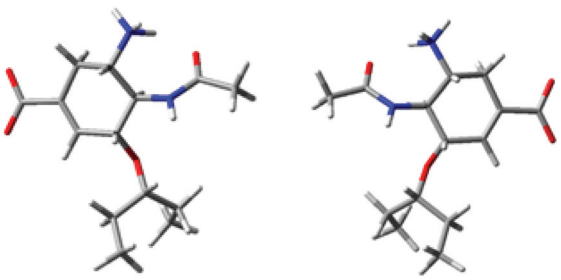

I. (3*R*,4*R*,5*S*)-**7** II. (3*S*,4*S*,5*R*)-**7**

Fig. 3 3D-Structures of two enantiomers of oseltamivir carboxylate form mirror images with identical total energies.

pseudo-axial positions, while the 4-*N*-acetyl group is in the pseudo-equatorial position (Fig. 4). This configuration allows the formation of two intramolecular hydrogen bonds between the carbonyl oxygen of the 4-*N*-acetyl and hydrogen of the 5-amino group (an interatomic distance of 1.67 Å) and between oxygen of the 3-oxypentyl group and hydrogen of the 5-amino group (2.11 Å). On the other hand, the 1.8 kcal mol^{-1} less stable stereoisomers I, (3*R*,4*R*,5*S*)-7, and II, (3*S*,4*S*,5*R*)-7, of

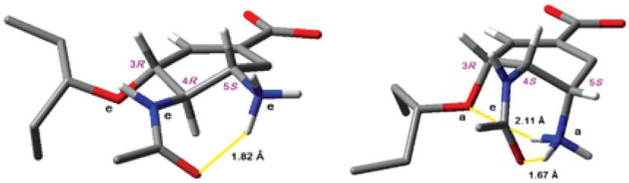

I. (3*R*,4*R*,5*S*)-**7**, $^5H_4$ ring puckering VI. (3*R*,4*S*,5*S*)-**7**, $^4H_5$ ring puckering

Fig. 4 3D-Structure, cyclohexene ring puckering and intramolecular hydrogen bonding pattern in oseltamivir stereoisomers (hydrogen bonds are shown as yellow lines, some nonpolar hydrogens are not shown for better clarity, a – axial, e – equatorial).

the oseltamivir carboxylate also form $^5H_4$ and $^4H_5$ half-chair ring conformations, however, with all three hetero-substituents being placed in pseudo-equatorial positions (Table 1, Fig. 4). In this configuration, only one hydrogen bond between the carbonyl oxygen of the 4-*N*-acetyl and hydrogen of the 5-amino group (1.82 Å) can be formed, which results in a lower predicted stability of these stereoisomers. Similar observation was made by Sartori *et al.*,[12] who determined from a metadynamics simulation that the free energy difference between stereoisomers I, (3*R*,4*R*,5*S*)-7, and VI, (3*R*,4*S*,5*S*)-7, of oseltamivir is of the order of 1 kcal mol^{-1}.

To determine the absolute configuration of chiral compounds, theoretical prediction of electronic CD spectra (ECD) is frequently used.[16] We have used a time-dependent DFT method to derive the ECD spectra of eight stereoisomers of oseltamivir. These theoretical ECD spectra were compared with the experimental spectrum of oseltamivir phosphate in water published by Górecki, Table 2 and Fig. 5.[17]

Comparison of the shape of the constituent circular dichroism Cotton effects suggested that the experimental ECD spec-

Table 2 Characteristic peaks in the experimental and computed ECD spectra of stereoisomers of oseltamivir in water

Stereoisomer	$\Delta\varepsilon$ [a] (dm^3 mol^{-1} cm^{-1})	λ_{max} [b] (nm)
I. (3*R*,4*R*,5*S*)-7·H_3PO_4 [c]	5.8	191
	−9.8	224
	2.6	253
I. Zwitterionic (3*R*,4*R*,5*S*)-7[d]	12	190
	−7	230
	3	290
V. Zwitterionic (3*S*,4*R*,5*R*)-7[d]	−25	190
	37	220
	−3	250
VI. Zwitterionic (3*R*,4*S*,5*S*)-7[d]	25	190
	−37	220
	3	250

[a] $\Delta\varepsilon$ – molar circular dichroism. [b] λ_{max} – wavelength of peak. [c] ECD spectrum in water recorded by Górecki.[17] [d] ECD spectrum computed by time-dependent DFT method (TDDFT-B3LYP-SCRF/6-31+G*) in water.[15]

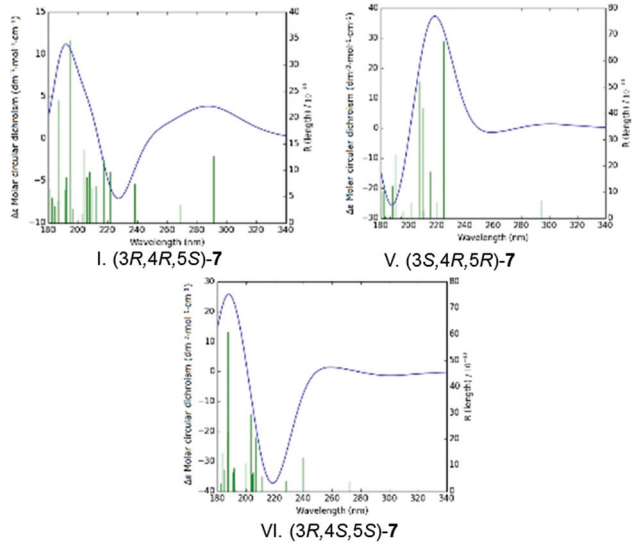

Fig. 5 Computed ECD spectra for three stereoisomers of oseltamivir carboxylate.

Table 3 Predicted relative binding affinities ($\Delta\Delta E_{bin,sol}$) of stereoisomers of oseltamivir carboxylate to neuraminidase N1[a] of influenza A virus[b]

Stereoisomer	$\Delta\Delta E_{bin,sol}$ [c] [kcal mol^{-1}]
I. (3*R*,4*R*,5*S*)-7[d]	0
II. (3*S*,4*S*,5*R*)-7	27
III. (3*S*,4*R*,5*S*)-7	−32
IV. (3*R*,4*S*,5*R*)-7	54
V. (3*S*,4*R*,5*R*)-7	12
VI. (3*R*,4*S*,5*S*)-7	4
VII. (3*S*,4*S*,5*S*)-7	−87
VIII. (3*R*,4*R*,5*R*)-7	1

[a] Crystal structure of neuraminidase of type N1 was taken from *Protein Data Bank* (PDB entry 2HU0[23]). [b] Influenza virus – A/Viet Nam/1203/2004(H5N1). [c] $\Delta\Delta E_{bin,sol}$ – relative differences in binding energies were computed as:[19] $\Delta\Delta E_{bin,sol} = (\Delta E_{tot,sol}[N1:O_i] - \Delta E_{tot,sol}[N1] - \Delta E_{tot,sol}[O_i]) - \Delta E_{bin,sol,Ref}$ for optimized solvated molecular geometries of oseltamivir carboxylate stereoisomers [O_i], enzyme : oseltamivir complexes [$N1:O_i$] and enzyme [N1] using QSite[18b] at the DFT-B3LYP-PBSA/6-31+G*:OPLS-2005 level of theory. [d] Configuration of stereoisomer I. (3*R*,4*R*,5*S*) of oseltamivir carboxylate, which corresponds to the absolute configuration of Tamiflu, was used as the reference.

trum of oseltamivir phosphate recorded in water[17] matches with the calculated spectrum of VI, (3*R*,4*S*,5*S*)-7, and, to some extent, also the spectrum of stereoisomer I with the configuration (3*R*,4*R*,5*S*)-7 identical to that of Tamiflu.

Computational prediction of binding affinity of individual stereoisomers of oseltamivir carboxylate to the viral neuraminidase N1 subtype of the influenza A virus (A/Viet Nam/1203/2004(H5N1), PDB entry 2HU0 [30]) was carried out by docking of the inhibitors to the active site in the relaxed crystal structure of N1. Then, the hybrid quantum mechanical/molecular mechanical (QM/MM) method[18] was employed to derive the binding energy of inhibitors to the relaxed enzyme using a supermolecular approach described by Frecer *et al.*[19] Eleven amino acid residues surrounding the bound inhibitor, oseltamivir itself and two structural water molecules were included into the quantum motif, while the remaining 376 residues present in the crystal structure of the viral neuraminidase were described by molecular mechanics and an OPLS-2005 force field.[18b,20]

The predicted relative binding affinities in solution ($\Delta\Delta E_{bin,sol}$) of stereoisomers of oseltamivir carboxylate to the neuraminidase N1 (Table 3) indicate, as expected, that the enzyme inhibition is stereospecific. Moreover, they suggest that binding of the two stereoisomers of oseltamivir to N1 will be stronger than that of the active metabolite of Tamiflu I, (3*R*,4*R*,5*S*)-7-oseltamivir. The calculations predict that the stereoisomers of oseltamivir will inhibit the neuraminidase N1 of the influenza A virus in the following descending order:

VII, (3*S*,4*S*,5*S*)-7 > III, (3*S*,4*R*,5*S*)-7 > I, (3*R*,4*R*,5*S*)-7 > > VIII, (3*R*,4*R*,5*R*)-7 > VI, (3*R*,4*S*,5*S*)-7 > V, (3*S*,4*R*,5*R*)-7 > > II, (3*S*,4*S*,5*R*)-7 > IV, (3*R*,4*S*,5*R*)-7

According to the calculations (Table 3), the two stereoisomers of oseltamivir VII, (3*S*,4*S*,5*S*)-7, and III, (3*S*,4*R*,5*S*)-7, can be expected to inhibit neuraminidase N1 stronger than the Tamiflu itself. Relatively high differences in the calculated $\Delta\Delta E_{bin,sol}$ are related to the binding of polar oseltamivir stereoisomers (zwitterions) to a highly polar binding site of the enzyme (6 cationic and 5 anionic residues and 2 water molecules within 4 Å distance from the bound ligand). Therefore, even small changes in the molecular structure and geometry may result in relatively large changes of the electrostatic component of the interaction energy and solvation energies. In addition, chirality of the three stereocenters in combination with the cyclohexene ring puckering and oseltamivir recognition orients the heterosubstituents in different directions, which results in close contacts with different residues of the N1 binding site (Fig. 6 and 7).

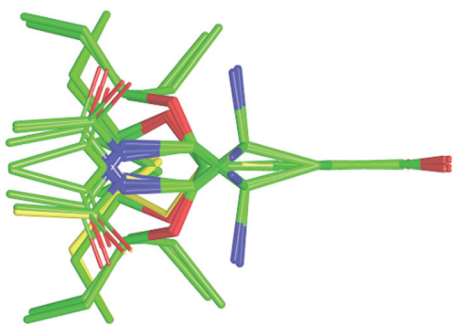

Fig. 6 Superimposed structures of 8 stereoisomers of oseltamivir carboxylate docked to the binding site of N1. Hydrogen atoms are not shown. The carboxylic group of oseltamivir (on the right) is recognized by and strongly interacts with 3 arginines (Arg118, Arg292 and Arg371, Fig. 7).[21] This interaction defines its position and orientation at the N1 binding site, it also co-determines relative positions of the heterosubstituents. Side view of the superimposed molecules with the cyclohexene ring double bond and the carboxylic group C2═(C1–COO^-)–C6 positioned in the horizontal plane. Stereoisomer I, (3*R*,4*R*,5*S*)-7-oseltamivir, is shown in yellow color.

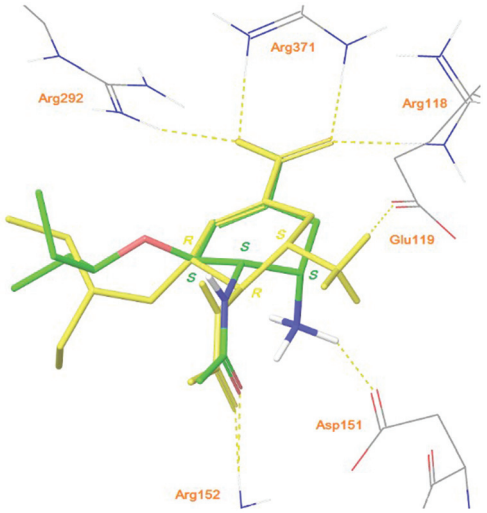

Fig. 7 Superimposed structures of two stereoisomers of oseltamivir carboxylate I, (3*R*,4*R*,5*S*)-**7**, (yellow color) and VII, (3*S*,4*S*,5*S*)-**7**, docked to N1 binding site and optimized by QM/MM method.[18] Yellow dashed lines represent intermolecular hydrogen bonds. Nonpolar hydrogens were omitted for better clarity.

Inspection of enzyme-inhibitor interactions at the active site of N1 shows that the major differences in the inhibitor binding between stereoisomers VII, (3*S*,4*S*,5*S*)-7, and I, (3*R*,4*R*,5*S*)-7, occur in the hydrogen bonding pattern at the 5-amino group (Fig. 7).

The calculations suggest that the synthesized stereoisomer (3*S*,4*R*,5*S*)-**1** of oseltamivir (Fig. 1) or III, (3*S*,4*R*,5*S*)-7, oseltamivir carboxylate (Table 3) should represent a more potent inhibitor of neuraminidase N1 compared to the active metabolite of Tamiflu. Whether this prediction will be carried over also to the *in vitro* antiviral effect on the influenza virus infected cells was determined in biological tests.

Biological evaluation

The antiviral efficacy of three stereoisomers ((3*R*,4*R*,5*R*)-7, (3*S*,4*R*,5*S*)-7, and (3*S*,4*R*,5*R*)-7) of oseltamivir carboxylate ((3*R*,4*R*,5*S*)-7), prepared by using the above described procedures, has been examined *in vitro* by a rapid culture assay (RCA) on MDCK cells using the influenza A virus of a H3N2 subtype and Tamiflu resistant/sensitive variants of pandemic 2009 virus of a H1N1 subtype. The most significant inhibition of virus replication A/Miss (H3N2) (>90%) has been measured using the virus dose of 34 pfu per 100 μl per well at the 39.06 nM concentration of compound (3*R*,4*R*,5*S*)-7-oseltamivir. All other compounds revealed lower inhibition efficacy (Table 4 and Fig. 8). The inhibition of virus replication by 50% allowed the differentiation of antiviral potential of these compounds in the following sequence: (3*R*,4*R*,5*S*)-7 > (3*R*,4*R*,5*R*)-7 > (3*S*,4*R*,5*S*)-7 > (3*S*,4*R*,5*R*)-7.

To learn whether some of the above mentioned stereoisomers inhibit replication of Tamiflu-resistant influenza A viruses, we used Tamiflu-sensitive and Tamiflu-resistant variants of the human pandemic 2009 virus A/Perth of the H1N1 subtype (TSV-A/Perth and TRV-A/Perth). The replication of TRV-A/Perth virus was inhibited only up to 60% at the highest tested concentration (*i.e.* at 5000 nM) of (3*R*,4*R*,5*S*)-7-oseltamivir-carboxylate and none of the examined stereoisomers exceeded its inhibition efficacy at 5000 nM (Table 5). No inhibition of TRV virus occurred at 625 nM concentration of oseltamivir stereoisomers. In contrast, all the tested compounds in the used concentration range inhibited the replication of TSV-A/Perth virus. The order of substances according to their antiviral efficacy against TSV-A/Perth was the same as was

Table 4 Efficacy of inhibition of A/Mississippi/1/85(H3N2) virus replication by tested compounds

	Concentration of tested substance (nM)	
Tested substance	90% virus inhibition	50% virus inhibition
(3*R*,4*R*,5*S*)-7	39.1	1.22
(3*R*,4*R*,5*R*)-7	1250	9.76
(3*S*,4*R*,5*S*)-7	5000	39.1
(3*S*,4*R*,5*R*)-7	5000	78.1

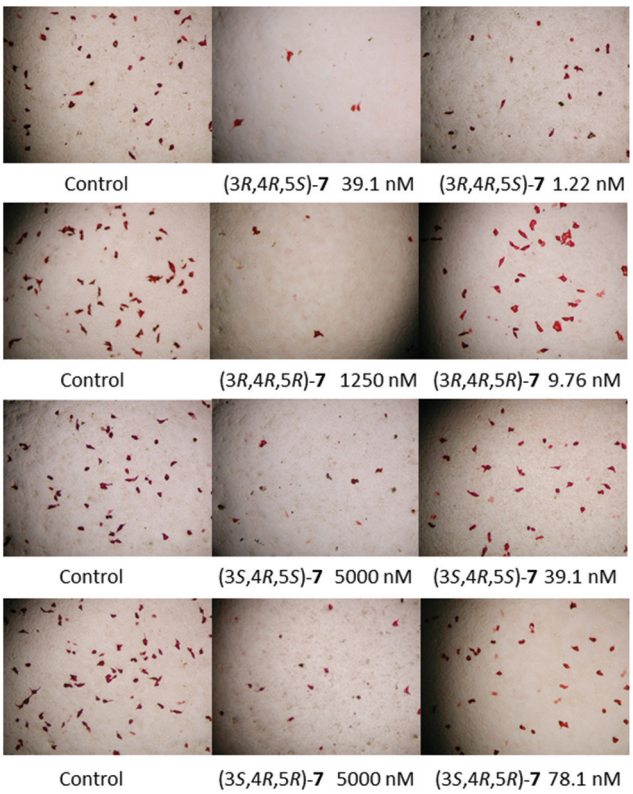

Fig. 8 Comparison of *in vitro* antiviral efficacy of oseltamivir and its stereoisomers. Examination of antiviral effects of compounds (3*R*,4*R*,5*S*)-7, (3*R*,4*R*,5*R*)-7, (3*S*,4*R*,5*S*)-7, and (3*S*,4*R*,5*R*)-7 compared to the virus control (no inhibitor) by RCA on the replication of influenza virus A/Mississippi/1/85 (H3N2). MDCK cells were infected by virus dose 34 pfu per sample. Left column: control-0% inhibition of virus replication, medium column-≥90% inhibition, right column-50% inhibition.

Table 5 Inhibition of TSV-A/Perth virus and TRV-A/Perth virus replication by tested compounds

	Inhibition of replication (%)			
	TSV-A/Perth virus[a]		TRV-A/Perth virus[b]	
Compound	5000 nM[c]	625 nM[c]	5000 nM[c]	625 nM[c]
(3*R*,4*R*,5*S*)-7	100	90	60	50
(3*R*,4*R*,5*R*)-7	100	80	50	0
(3*S*,4*R*,5*S*)-7	100	85	10	0
(3*S*,4*R*,5*R*)-7	100	60	0	0

[a] TSV – Tamiflu-sensitive virus. [b] TRV – Tamiflu-resistant virus. [c] Concentration of tested substance.

with A/Miss virus. Their antiviral efficacy on A/Perth virus replication descended equally as in the case of A/Miss, *i.e.* from (3*R*,4*R*,5*S*)-7, which was the most efficient, to (3*S*,4*R*,5*R*)-7, the antiviral efficacy of which was the lowest.

Conclusions

We have described stereoselective synthesis, computational evaluation and biological testing of three, so far unknown and untested, diastereoisomers of oseltamivir. These isomers have been synthesized using stereoselective organocatalytic Michael addition, followed by cyclization *via* another Michael addition and Horner–Wadsworth–Emmons reaction. The last step in the synthesis was nitro group reduction, which afforded stereoisomers of oseltamivir, or after basic hydrolysis free carboxylates for biological testing. Binding affinities of these derivatives to neuraminidase N1 (A/Viet Nam/1203/2004(H5N1)) were studied by computational methods using a combination of DFT and molecular mechanics calculations. According to these calculations two stereoisomers of oseltamivir showed even greater binding affinity to the N1 neuraminidase than oseltamivir itself. *In vitro* antiviral assays revealed that all three synthesized isomers have antiviral activity, but it was lower than that of oseltamivir. However, the stereoisomer III, (3*S*,4*R*,5*S*)-7, with predicted elevated inhibitory activity against neuraminidase N1 showed *in vitro* inhibitory potency towards the Tamiflu-sensitive viral strain A/Perth/265/2009(H1N1) comparable to Tamiflu. Further research of the remaining stereoisomers of oseltamivir is underway in our laboratories.

Experimental

Synthesis

The solvents were purified by standard methods.[22] Commercially available chemicals were used without further purification. NMR spectra were recorded on a Varian NMR System 300 or 600 instrument (300 MHz for ^{1}H, 151 MHz for ^{13}C). Chemical shifts (δ) are given in ppm relative to tetramethylsilane. Specific optical rotations were measured on a Jasco P-2000 instrument and are given in deg cm^3 g^{-1} dm^{-1}. Column chromatography was performed on silica gel 60A (0.04–0.6 mm). Thin-layer chromatography was performed on the Merck TLC-plates silica gel 60, F-254. Enantiomeric excesses were determined by HPLC using Chiralpak and Chiralcel columns (Daicel Chemical Industries) using *n*-hexane/propan-2-ol as a mobile phase and UV detection.

Synthetic procedures and characterization data

2-(Pentan-3-yloxy)acetaldehyde (2). DIBAL (800 mL, 962 mmol, 20 wt% in hexane) was added dropwise into a cooled solution of pentan-3-ol (97.8 g, 1.11 mol, 115 mL) in CH_2Cl_2 (540 mL) at 0 °C for 40 min. The solution was stirred for 30 min at 5 °C and then for 30 min at room temperature. Subsequently, oxiran-2-ylmethanol (54.8 g, 740 mmol, 48.9 mL) was added into the reaction mixture which was stirred at room temperature for 96 h. The reaction was stopped by pouring the reaction mixture into ice with concentrated HCl. The solution was washed with a saturated solution of NaCl after being warmed at room temperature. After extraction by EtOAc, the organic layers were dried over Na_2SO_4. The solid phase was filtered off and the filtrate was concentrated under vacuum. The crude reaction mixture was purified by reduced pressure distillation (T = 85 °C, 1.2 mbar) to provide 3-(pentan-3-yloxy)propane-1,2-diol as a colorless oil; yield 23.4 g (19.5%). ^{1}H NMR (300 MHz, $CDCl_3$): δ 3.89–3.79 (m, 1H), 3.77–3.44 (m, 4H), 3.17 (quint., J = 5.8 Hz, 1H), 2.98 (br s, 1H), 2.75 (br s, 1H), 1.60–1.43 (m, 4H), 0.96–0.83 (m, 6H). ^{1}H NMR data agree with those in the literature.[8b] ^{13}C NMR (75 MHz, $CDCl_3$): δ 82.7, 70.6, 70.2, 64.2, 25.7, 9.5.

The solution of $NaIO_4$ in water (5.56 g, 26.0 mmol dissolved in 28 mL water) was added dropwise into the mixture of silica gel (50.0 g) in CH_2Cl_2 (260 mL). The resulting mixture was stirred for 15 min at RT. 3-(Pentan-3-yloxy)propane-1,2-diol (3.24 g, 20.0 mmol) in CH_2Cl_2 (20 mL) was added into the reaction mixture. The mixture was stirred at room temperature for 3 h. Subsequently, the silica gel from the reaction mixture was filtered off over frit. The filtrate was washed with a saturated solution of $Na_2S_2O_3$. The solvent was evaporated under reduced pressure and the crude reaction mixture was purified by distillation under reducer pressure (T = 55 °C, 12 mbar) to provide a colorless oil; yield 1.8 g (69%).

^{1}H NMR (300 MHz, $CDCl_3$): δ 9.76 (t, J = 1.1 Hz, 1H), 4.06 (d, J = 1.1 Hz, 2H), 3.23 (quint, J = 5.8 Hz, 1H), 1.56 (dq, J = 7.6 Hz, 3.2 Hz, 4 H), 0.93 (t, J = 7.4 Hz, 6H). ^{1}H NMR data agree with those in the literature.[7a] ^{13}C NMR (75 MHz, $CDCl_3$): δ201.7, 83.5, 74.5, 25.6, 9.4.

(*Z*)-2-Nitroethen-1-amine. A mixture of nitromethane (122 g, 2.0 mol, 108 mL), *N*-methylaniline (42.9 g, 400 mmol, 43.3 mL), PTSA (2 g, 10.5 mmol) and (diethoxymethoxy)ethane (119 g, 800 mmol, 133 mL) was refluxed for 8 h under an inert atmosphere (Ar). The reaction was cooled at room temperature and stirred overnight. At the end the reaction was complete by solvent evaporating from the reaction mixture under reduced pressure. Hexane (200 mL) was slowly added into the concentrated mixture and *N*-methyl-*N*-[(*E*)-2-nitroethenyl]aniline began to crystallize. The precipitate was filtered off, washed

with hexane (100 mL) and dried under reduced pressure for 60 min at 40 °C. *N*-Methyl-*N*-[(*E*)-2-nitroethenyl] aniline was obtained as a pale yellow crystalline substance; yield 53 g (74%).

mp = 89.4–91.1 °C (94 °C).[23] ^{1}H NMR (300 MHz, $CDCl_3$): δ 8.49 (d, J = 11 Hz, 1H), 7.62–7.14 (m, 5H), 6.85 (d, J = 10.9 Hz, 1H), 3.34 (s, 3H). ^{13}C NMR (75 MHz, $CDCl_3$): δ 147.2, 129.9, 126.4, 120.8, 116.5, 77.1. Spectral data corresponds with the literature.[24]

N-Methyl-*N*-[(*E*)-2-nitroethenyl]aniline (21.0 g, 118 mmol) was dissolved in $CHCl_3$ (430 mL). The mixture was cooled to 0 °C and saturated with gaseous NH_3 (14.7 g, 861 mmol) for 1 h at a temperature ranging from 0 °C to 5 °C. The final saturated mixture was stored in a refrigerator overnight. The crystals were filtered off next day and washed with $CHCl_3$. The crystalline substance was dried under reduced pressure at room temperature to provide a beige colored crystalline substance; yield 9.5 g (91%).

Mp = 100.1–101.2 °C (101 °C).[13] ^{1}H NMR (300 MHz, $CDCl_3$): δ 8.44 (br s, 1H), 6.87–6.70 (m, 1H), 6.48 (d, J = 6.0 Hz, 1H), 5.65 (br s, 1H). ^{1}H NMR data agree with those in the literature.[8b] ^{13}C NMR (75 MHz, DMSO): δ 151.2, 147.1 (CH(*Z*)), 114.0, 109.7 (CH(*E*)) (Note: 2-nitroethen-1-amine isomerizes in polar solvents to a mixture of *E* and *Z*-isomer).

***N*-[(*Z*)-2-Nitroethenyl]acetamide (3).** Pyridine (8.26 g, 104 mmol, 8.4 mL) and acetic anhydride (5.33 g, 52.2 mmol, 4.94 mL) were added into a cooled mixture of (*Z*)-2-nitroethen-1-amine (2.30 g, 26.1 mmol) and DMAP (0.64 g, 5.22 mmol) at 0 °C. The reaction mixture was warmed to room temperature and stirred overnight. The reaction was complete on dilution with CH_2Cl_2 (100 mL), washing with distillated water (2 × 100 mL), and then with NaCl saturated solution (150 mL). The organic layers were dried over Na_2SO_4. The solvent was evaporated and the crude reaction mixture was purified by column chromatography (SiO_2, hex/EtOAc 1 : 1) to provide a beige colored crystalline substance; yield 2.3 g (67%).

Mp = 109–113 °C (106–107 °C).[8a] ^{1}H NMR (300 MHz, $CDCl_3$): (*Z*)-isomer δ 10.40 (s, 1H), 7.59 (dd, J = 12.0 Hz, 6.9 Hz, 1H), 6.61 (d, J = 6.9 Hz, 1H), 2.28 (s, 3H). ^{1}H NMR data for *cis*-isomer agree with those in the literature.[14] ^{13}C NMR (75 MHz, DMSO): (*Z*)-isomer δ 168.3, 131.4, 118.5, 23.7.

^{1}H NMR (300 MHz, DMSO): mixture (*Z*)/(*E*) δ 11.09 (br s, $2H_{cis/trans}$), 8.27 (d, J = 12 Hz, $1H_{trans}$), 7.59 (d, J = 7 Hz, $1H_{cis}$), 7.32 (d, J = 12 Hz, $1H_{trans}$), 6.75 (d, J = 7 Hz, $1H_{cis}$), 2.26 (s, $1H_{cis}$), 2.12 (s, $3H_{trans}$).

Ethyl-2-(diethoxyphosphoryl)prop-2-enoate (4). A solution of formaldehyde (46.7 g, 560 mmol, 42.5 ml, 36% in H_2O) with piperidine (2.55 g, 30.3 mmol, 2.97 mL) was refluxed in MeOH (600 mL) for 30 min. Ethyl-2-(diethoxyphosphoryl) acetate (44.8 g, 200 mmol, 40 mL) was added into the reaction mixture at room temperature. The mixture was refluxed for next 65 h. Piperidine (0.5 mL) was added into the RM after 24 h and 48 h. The solvent was evaporated from the RM under reduced pressure. Subsequently, the crude product was diluted with $CHCl_3$ (100 mL) and extracted with $CHCl_3$. The organic layers were dried over Na_2SO_4. The solvent was evaporated under reduced pressure. H_3PO_4 (4 mL, conc.) was added into the crude product and it was purified by vacuum distillation (T = 90 °C, 0.3 mbar) to provide compound **4** as a colorless liquid; yield 20 g (42%).

^{1}H NMR (300 MHz, $CDCl_3$): δ 7.00 (dd, J = 42.0, 1.8 Hz, 1H), 6.75 (dd, J = 20.4, 1.8 Hz, 1H), 4.29 (q, J = 7.1 Hz, 2H), 4.25–4.08 (m, 4H), 1.41–1.29 (m, 9H). ^{13}C NMR (75 MHz, $CDCl_3$): δ 163.6 (d, $J_{P,C}$ = 15.8 Hz), 143.1 (d, $J_{P,C}$ = 4.7 Hz), 133.2 (d, $J_{P,C}$ = 185.8 Hz), 63.5 (d, $J_{P,C}$ = 5.9 Hz), 62.6 (d, $J_{P,C}$ = 5.9 Hz), 61.4, 16.2 (d, $J_{P,C}$ = 6.2 Hz), 13.9. Spectral data agree with those in the literature.[14]

***N*-[(2*R*,3*R*)-1-Nitro-4-oxo-3-(pentan-3-yloxy)butan-2-yl]acetamide (5).** 2-(Pentan-3-yloxy)acetaldehyde (**2**) (2.83 g, 21.8 mmol, 2.83 mL), cooled water (47 mL), mandelic acid (441 mg, 2.90 mmol) and a cooled solution of (2*S*)-2-(diphenyl[(trimethylsilyl)oxy] methyl)pyrrolidine (**C1**) (472 mg, 1.45 mmol) in 5 mL $CHCl_3$ were added into a suspension of *N*-[(*Z*)-2-nitroethenyl]acetamide (**3**) (1.89 g, 14.5 mmol) in $CHCl_3$ (42 mL) at 0 °C. The reaction mixture was stirred for 2 h at 0 °C. The reaction was stopped by adding saturated solution of NH_4Cl into the reaction mixture. The mixture was stirred for 15 min and extracted with $CHCl_3$. Organic layers were dried over Na_2SO_4. The solvent was evaporated under reduced pressure. The crude product was purified by column chromatography (SiO_2, hex/EtOAc 1 : 1) to provide compound **5** as a pale yellow oil – a mixture of isomers 1 : 1 (*syn*/*anti*); yield 2.5 g (65%). Diastereoisomers were isolated: (2*R*,3*R*) isomer 96% purity (dr 1 : 28 *syn*/*anti*, er 98 : 2); (2*R*,3*S*) isomer 89% purity (dr 8 : 1 *syn*/*anti*, er 97 : 3).

(2*R*,3*S*)-5 isomer: $[\alpha]_D^{23}$ = +1.1 (c = 1.0, $CHCl_3$, 17 : 1 *syn*/*anti*). ^{1}H NMR (300 MHz, $CDCl_3$): δ 9.64 (s, 1H), 6.09 (d, J = 8.7 Hz, 1H), 5.13–4.97 (m, 1H), 4.58 (d, J = 6.6 Hz, 2H), 4.09 (d, J = 3.3 Hz, 1H), 3.40 (quint., J = 5.8 Hz, 1H), 1.99 (s, 3H), 1.64–1.42 (m, 4H), 0.95 (d, J = 5.6 Hz, 3H), 0.90 (d, J = 5.6 Hz, 3H). ^{13}C NMR (75 MHz, $CDCl_3$): δ 201.1, 170.2, 83.6, 79.7, 74.2, 48.2, 26.0, 25.1, 23.1, 9.5, 9.4. Spectral data agree with those in the literature.[25]

(2*R*,3*R*)-5 isomer: $[\alpha]_D^{23}$ = +50.3 (c = 1.0, $CHCl_3$, 1 : 23 *syn*/*anti*). ^{1}H NMR (300 MHz, $CDCl_3$): δ 9.60 (d, J = 3.1 Hz, 1H), 6.18 (d, J = 8.3 Hz, 1H), 4.91–4.67 (m, 2H), 4.63–4.46 (m, 1H), 3.93 (dd, J = 8.0, 3.1 Hz, 1H), 3.35–3.19 (m, 1H), 2.00 (s, 3H), 1.63–1.36 (m, 4H), 0.97–0.81 (m, 6H). ^{13}C NMR (75 MHz, $CDCl_3$): δ 201.2, 170.6, 83.2, 80.5, 74.2, 47.3, 26.1, 24.9, 23.1, 9.5, 9.2. Spectral data agree with those in the literature.[25] HPLC: (Chiralpak OD-H column, 259 nm, hexane/iPro 85 : 15, 0.75 mL min^{-1}) $t_{R(syn\text{-major})}$ 28.6 min, $t_{R(syn\text{-minor})}$ 16.6 min; $t_{R(anti\text{-major})}$ 12.7 min, $t_{R(anti\text{-minor})}$ 10.5 min.

Ethyl-(3*R*,4*R*,5*S*)-4-acetamido-5-nitro-3-(pentan-3-yloxy)cyclohex-1-ene-1-carboxylate and ethyl-(3*R*,4*R*,5*R*)-4-acetamido-5-nitro-3-(pentan-3-yloxy)cyclohex-1-ene-1-carboxylate (6). K_2CO_3 (514 mg, 3.65 mmol) was added into a mixture of *N*-[(2*R*,3*S*)-1-nitro-4-oxo-3-(pentan-3-yloxy)butan-2-yl]acetamide (**5**) (395 mg, 1.52 mmol), ethyl-2-(diethoxyphosphoryl)prop-2-enoate (**4**) (412 mg, 1.75 mmol), and 18-crown-6 ether (44.6 mg, 0.167 mmol) in CH_2Cl_2 (20 mL), which was placed into a microwave reactor. The reaction was stirred under microwave irradiation at 70 °C for 2 h. The reaction was stopped by

adding NH_4Cl into the reaction mixture and extracted with CH_2Cl_2. Organic layers were dried over Na_2SO_4. The solvent was evaporated and the crude product was purified by column chromatography (SiO_2, hex/EtOAc 2 : 1) to provide compound **6** as a pale yellow oil as a mixture of isomers 2 : 1 (5*R*/5*S*); yield 337 mg (65%). The mixture of isomers was separated. The separated isomers were isolated as colorless solid substances.

(3*R*,4*R*,5*S*)-6 isomer: mp = 149.8–154.0 °C; $[\alpha]_D^{20} = -33.3$ (c = 1.0, $CHCl_3$). ^{1}H NMR (300 MHz, $CDCl_3$): δ 6.87–6.81 (m, 1H), 5.78 (br d, J = 6.7 Hz, 1H), 5.62 (ddd, J = 11.2, 10.5, 6.0 Hz, 1H), 4.95–4.70 (m, 1H), 4.23 (q, J = 7.1 Hz, 2H), 3.78–3.67 (m, 1H), 3.34 (quint., J = 5.7 Hz, 1H), 3.18–3.06 (m, 1H), 2.97–2.78 (m, 1H), 1.97 (s, 3H), 1.56–1.41 (m, 4H), 1.30 (t, J = 7.1 Hz, 3H), 0.98–0.82 (m, 6H). ^{13}C NMR (75 MHz, $CDCl_3$): δ 171.3, 165.3, 138.1, 126.9, 82.3, 82.1, 71.9, 61.5, 56.1, 29.6, 26.3, 25.6, 23.6, 14.3, 9.7, 9.4. Spectral data corresponds with the literature.[9b,26]

(3*R*,4*R*,5*R*)-6 isomer: mp = 135.3–139.8 °C; $[\alpha]_D^{20} = -58.8$, (c = 0.4, $CHCl_3$). ^{1}H NMR (300 MHz, $CDCl_3$): δ 6.91–6.84 (m, 1H), 5.71 (br d, J = 8.3 Hz, 1H), 4.99 (td, J = 6.9, 3.3 Hz, 1H), 4.78 (ddd, J = 8.3, 5.0 Hz, 3.4 Hz, 1H), 4.25 (q, J = 7.1 Hz, 1H), 4.17–4.04 (m, 1H), 3.61–3.39 (m, 1H), 3.09–2.95 (m, 2H), 1.99 (s, 3H), 1.66–1.42 (m, 4H), 1.31 (t, J = 7.1 Hz, 3H), 0.96 (t, J = 7.4 Hz, 3H), 0.90 (t, J = 7.4 Hz, 3H). ^{13}C NMR (75 MHz, $CDCl_3$): δ 169.4, 164.4, 134.5, 127.7, 81.8, 79.3, 71.4, 60.6, 49.2, 25.6, 25.4, 24.7, 22.4, 13.3, 8.9, 8.4. Spectral data corresponds with the literature.[9b,26] HPLC (Chiralcel AD-H column, 230 nm, hexane/iPro 93 : 7, 0.5 mL min^{-1}) $t_{R(5S\text{-major})}$ 41.5 min, $t_{R(5S\text{-minor})}$ 26.1 min, $t_{R(5R\text{-major})}$ 18.2 min, $t_{R(5R\text{-minor})}$ 17.5 min.

Ethyl-(3*R*,4*R*,5*S*)-4-acetamido-5-amino-3-(pentan-3-yloxy)cyclohex-1-ene-1-carboxylate (1, oseltamivir). Chlorotrimethylsilane (167 mg, 1.54 mmol, 0.19 mL) was added into a flask with zinc powder (1.30 g, 20 mmol) and dry ether (35 mL). The mixture was stirred for 15 min at room temperature under an inert atmosphere. Activated zinc was filtered under an inert atmosphere (Ar), washed with dry ether (2 × 10 mL). Ethyl-(3*R*,4*R*,5*S*)-4-acetamido-5-nitro-3-(pentan-3-yloxy)cyclohex-1-ene-1-carboxylate (**6**) (263 mg, 0.77 mmol) and acetic acid (15.6 mg, 260 mmol, 14.9 mL) were added into the flask with activated zinc. The mixture was stirred under reflux for 8 h. Zinc was filtered off and washed with EtOAc. The filtrate was concentrated under reduced pressure. The worked reaction mixture was purified by column chromatography (SiO_2, EtOAc/MeOH 2 : 1) to provide compound **7** as a colorless solid substance; yield 134 mg (56%).

HRMS m/z $[M + H]^+$ calculated: 313.213, measured: 312.212, mp = 90.2–92.1 °C (107–108 °C;[26] 102.5–103.9 °C (ref. 27)), $[\alpha]_D^{20} = -52.7$, (c = 1.03, $CHCl_3$), ($[\alpha]_D^{20} = -57.2$, c = 1, $CHCl_3$),[25] IR (neat): 3281s (N–H), 2922m (C–H), 1710s (C═O), 1630s (C═C), 1544 (N–H). ^{1}H NMR (300 MHz, $CDCl_3$): δ 6.79 (t, J = 2.1 Hz, 1H), 5.53 (br d, J = 7.6 Hz, 1H), 4.29–4.12 (m, 3H), 3.52 (dt, J = 10.3, 8.3 Hz, 1H), 3.35 (dd, J = 11.4, 5.7 Hz, 1H), 3.25 (ddd. J = 15.4, 10.1, 5.0 Hz, 1H), 2.75 (dd, J = 17.7, 5.3 Hz, 1H), 2.25–2.08 (m, 1H), 2.04 (s, 3H), 1.76 (br s, 2H), 1.62–1.41 (m, 4H), 1.34–1.23 (m, 3H), 0.90 (td, J = 7.4, 2.4 Hz, 6H). ^{13}C NMR (75 MHz, $CDCl_3$): δ 171.1, 166.5, 137.7, 129.6, 81.8, 74.9, 61.0, 59.1, 26.4, 25.8, 23.8, 14.3, 9.7, 9.5. Spectral data corresponds with the literature.[8a,b]

(3*R*,4*R*,5*S*)-4-Acetamido-5-amino-3-(pentan-3-yloxy)cyclohex-1-ene-1-carboxylic acid ((3*R*,4*R*,5*S*)-7). 1 M water solution of NaOH (27.5 mg, 0.69 mmol) was added into a flask with aminoester (3*R*,4*R*,5*S*)-**1** (135 mg, 0.43 mmol) dissolved in THF (14.2 mL) at 0 °C. The reaction mixture was stirred at 65 °C for 1 h. The reaction was complete after TLC detection by adding acidic amberlite (2 g). The mixture was stirred for next 15 min and subsequently amberlite was filtered off and washed with EtOH. The solvent was evaporated under reduced pressure and the worked reaction mixture was purified by flash chromatography (reverse column, acetonitrile/H_2O 19 : 1) to provide colorless powder; yield 20 mg (16%).

HRMS: m/z $[M + H]^+$ calculated: 285.182, measured: 285.181. mp = 187.2–191.9 °C (185–187 °C),[28] $[\alpha]_D^{20} = -21.4$ (c = 0.4, H_2O), ($[\alpha]_D^{20} = -143.2$, c = 0.4, H_2O),[28] IR (neat): 3362w (N–H), 2956m (C–H), 1630m (C═C), 1544s (N–H).

^{1}H NMR (300 MHz, D_2O): δ 6.53–6.50 (m, 1H), 4.30 (d, J = 8.9 Hz, 1H), 4.06 (dd, J = 11.6, 8.9 Hz, 1H), 3.60–3.51 (m, 2H), 2.90 (dd, J = 17.1, 5.5 Hz, 1H), 2.56–2.43 (m, 1H), 2.10 (s, 3H), 1.68–1.36 (m, 4H), 0.89 (dt, J = 14.4, 7.4 Hz, 6H). ^{13}C NMR (75 MHz, D_2O): δ 175.1, 173.7, 132.9, 132.5, 84.2, 75.6, 52.9, 49.7, 29.4, 25.4, 25.1, 22.3, 8.5, 8.4. Spectral data corresponds with the literature.[28]

Ethyl-(3*R*,4*R*,5*R*)-4-acetamido-5-amino-3-(pentan-3-yloxy)cyclohex-1-ene-1-carboxylate ((3*R*,4*R*,5*R*)-1). Chlorotrimethylsilane (204 mg, 1.88 mmol, 0.24 mL) was added into a flask with zinc powder (1.60 g, 24.4 mmol) and dry Et_2O (43 mL). The mixture was stirred for 15 min at room temperature under an inert atmosphere. Activated zinc was filtered under an inert atmosphere (Ar), and washed with dry Et_2O (2 × 10 mL). Ethyl-(3*R*,4*R*,5*R*)-4-acetamido-5-nitro-3-(pentan-3-yloxy)cyclohex-1-ene-1-carboxylate (322 mg, 0.94 mmol) and acetic acid (19.1 mg, 318 mmol, 18.2 mL) were added into the flask with activated zinc. The mixture was stirred at room temperature overnight. Zinc was filtered off and washed with EtOAc. The filtrate was concentrated under reduced pressure. The worked reaction mixture was purified by column chromatography (SiO_2, EtOAc/MeOH 2 : 1) to provide a colorless oil; yield 188 mg (64%).

HRMS: m/z $[M + H]^+$ calculated: 313.213, measured: 313.212, $[\alpha]_D^{23} = -53.1$ (c = 1, $CHCl_3$). ^{1}H NMR (300 MHz, $CDCl_3$): δ 6.86–6.76 (m, 1H), 6.21 (br d, J = 7.9 Hz, 1H), 4.22–4.15 (m, 3H), 4.00 (t, J = 4.0 Hz, 1H), 3.57 (br s, 2H), 3.53–3.44 (m, 2H), 2.74 (dd, J = 18.5, 5.3 Hz, 1H), 2.32–2.13 (m, 1H), 1.99 (s, 3H), 1.59–1.40 (m, 4H), 1.27 (t, J = 7.1 Hz, 3H), 0.89 (dt, J = 10.8, 7.4 Hz, 6H). ^{13}C NMR (75 MHz, $CDCl_3$): δ 171.4, 166.4, 135.1, 130.7, 82.0, 72.6, 61.1, 51.8, 45.6, 29.2, 26.50, 26.49, 23.53, 14.3, 10.1, 9.4.

(3*R*,4*R*,5*R*)-4-Acetamido-5-amino-3-(pentan-3-yloxy)cyclohex-1-ene-1-carboxylic acid ((3*R*,4*R*,5*R*)-7). 1 M water solution of KOH (20.2 mg, 0.36 mmol) was added into a flask with aminoester (3*R*,4*R*,5*R*)-**1** (56.2 mg, 0.18 mmol) dissolved in THF (5.7 mL) at 0 °C. The reaction mixture was stirred at room temperature for 3 h. The reaction was complete after TLC detection by adding acidic amberlite (1 g). The mixture was stirred for next 15 min and subsequently amberlite was filtered off and washed with EtOH. The solvent was evaporated under

reduced pressure and the worked reaction mixture was purified by flash chromatography (reverse column, acetonitrile/H_2O 19 : 1) to provide colorless powder; yield 21.3 mg (42%).

HRMS: m/z $[M + H]^+$ calculated: 285.181, measured: 285.180, mp = 151.1–156.5 °C, $[\alpha]_D^{20}$ = −54.3 (c = 0.4, D_2O), IR (neat): 3292w (N–H), 2963m (C–H), 1647m (C═C), 1539s (N–H). ^{1}H NMR (600 MHz, D_2O): δ 6.63–6.52 (m, 1H), 4.51–4.49 (m, 1H), 4.19–4.03 (m, 1H), 3.74 (ddd, J = 8.3, 5.5, 3.3 Hz, 1H), 3.62–3.54 (m, 1H), 2.84 (dd, J = 17.9, 5.6 Hz, 1H), 2.47–2.28 (m, 1H), 2.05 (s, 3H), 1.72–1.35 (m, 4H), 0.95 (t, J = 7.4 Hz, 3H), 0.90 (t, J = 7.5 Hz, 3H). ^{13}C NMR (75 MHz, $CDCl_3$): 175.4, 173.6, 136.4, 128.0, 83.0, 72.7, 47.9, 46.9, 25.9, 25.6, 25.4, 21.8, 9.5, 8.2.

Ethyl-(3*S*,4*R*,5*S*)-4-acetamido-5-nitro-3-(pentan-3-yloxy)cyclohex-1-ene carboxylate ((3*S*,4*R*,5*S*)-6) and ethyl-(3*S*,4*R*,5*R*)-4-acetamido-5-nitro-3-(pentan-3-yloxy)cyclohex-1-ene carboxylate ((3*S*,4*R*,5*R*)-6). K_2CO_3 (1.69 mg, 12.0 mmol) was added into a mixture of *N*-[(2*R*,3*R*)-1-nitro-4-oxo-3-(pentan-3-yloxy)butan-2-yl]acetamide (1.30 g, 5.0 mmol), ethyl-2-(diethoxyphosphoryl) prop-2-enoate (**4**) (1.36 g, 5.75 mmol), and 18-crown-6 ether (147 mg, 0.55 mmol) in CH_2Cl_2 (66 mL), which was placed into a microwave reactor. The reaction was stirred under microwave irradiation at 70 °C for 2 h. The reaction was stopped by adding NH_4Cl into the reaction mixture and extracted with CH_2Cl_2. Organic layers were dried over Na_2SO_4. The solvent was evaporated and the crude product was purified by column chromatography (SiO_2, hex/EtOAc 2 : 1) to provide a yellow oil as a mixture of isomers 4 : 1 (5*S*/5*R*); yield 950 mg (55%). The mixture of isomers was separated once more by column chromatography (SiO_2, CH_2Cl_2/EtOAc/CH_3CO_2H 9 : 1 : 0.05). The separated isomers were isolated in enantiomeric ratios 26 : 74 (3*S*,4*R*,5*R*) and 90 : 10 for the (3*S*,4*R*,5*S*) isomer.

(3*S*,4*R*,5*R*)-6 isomer: pale yellow oil, HRMS: m/z $[M + H]^+$ calculated: 343.187, measured: 343.186, $[\alpha]_D^{20}$ = +58.7, (c = 0.73, $CHCl_3$). ^{1}H NMR (300 MHz, $CDCl_3$) δ 6.97–6.91 (m, 1H), 6.44 (br d, J = 8.5 Hz, 1H), 4.78–4.71 (m, 1H), 4.71–4.61 (m, 1H), 4.26 (q, J = 7.1 Hz, 2 H), 4.17–4.10 (m, 1H), 3.40–3.25 (m, 2H), 2.66 (dd, J = 19.1, 3.4 Hz, 1H), 2.08 (s, 3H), 1.59–1.38 (m, 4H), 1.33 (t, J = 7.1 Hz, 3H), 0.91–0.76 (m, 6H). ^{13}C NMR (75 MHz, $CDCl_3$): δ 170.3, 165.7, 134.8, 129.1, 81.4, 79.2, 68.8, 61.5, 49.3, 27.1, 26.2, 25.7, 23.4, 14.3, 9.5, 9.3.

(3*S*,4*R*,5*S*)-6 isomer: colorless solid substance, HRMS: m/z $[M + H]^+$ calculated: 343.187, measured: 343.186, $[\alpha]_D^{20}$ = +93.5, (c = 1.002, $CHCl_3$), mp = 88.5 °C–95.8 °C. ^{1}H NMR (300 MHz, $CDCl_3$): δ 6.96–6.89 (m, 1H), 5.94 (br d, J = 8.6 Hz, 1H), 4.89 (dd, J = 16.8, 9.0 Hz, 1H), 4.80–4.59 (m, 1H), 4.23 (q, J = 7.1 Hz, 2H), 4.11 (t, J = 4.4 Hz, 1H), 3.43–3.27 (m, 1H), 3.17–2.95 (m, 2H), 1.98 (s, 3H), 1.60–1.40 (m, 4H), 1.30 (t, J = 7.1 Hz, 3H), 0.91 (t, J = 7.4 Hz, 3H), 0.85 (t, J = 7.4 Hz, 3H). ^{13}C NMR (75 MHz, $CDCl_3$): δ 170.1, 165.3, 134.9, 129.4, 81.9, 81.8, 69.5, 61.6, 50.3, 29.0, 26.6, 25.9, 23.3, 14.3, 9.7, 9.6. HPLC: (Chiralcel IA column, 230 nm, hexane/iPro 93 : 7, 0.75 mL min^{-1}): $t_{R(5S\text{-major})}$ 27.5 min, $t_{R(5S\text{-minor})}$ 21.1 min, $t_{R(5R\text{-minor})}$ 17.0 min, $t_{R(5R\text{-major})}$ 16.0 min.

Ethyl-(3*S*,4*R*,5*S*)-4-acetamido-5-amino-3-(pentan-3-yloxy)cyclohex-1-ene carboxylate ((3*S*,4*R*,5*S*)-1). Chlorotrimethylsilane (97.8 mg, 0.90 mmol, 0.11 mL) was added into a flask with zinc powder (765 mg, 11.7 mmol) and dry Et_2O (21 mL). The mixture was stirred for 15 min at room temperature under an inert atmosphere. Activated zinc was filtered under an inert atmosphere (Ar), washed with dry ether (2 × 10 mL). Ethyl-(3*S*,4*R*,5*R*)-4-acetamido-5nito-3-(pentan-3-yloxy)cyclohex-1-ene-1-carboxylate (154 mg, 0.45 mmol) and acetic acid (9.10 g, 152 mmol, 8.7 mL) were added into the flask with activated zinc. The mixture was stirred at room temperature overnight. Zinc was filtered off and washed with EtOAc. The filtrate was concentrated under reduced pressure. The worked reaction mixture was purified by column chromatography (SiO_2, EtOAc/MeOH 2 : 1) to provide colorless powder; yield 109 mg (77%).

HRMS: m/z $[M + H]^+$ calculated: 313.213, measured: 313.211, mp = 83.0–85.2 °C, $[\alpha]_D^{20}$ = +104.7, (c = 0.5, $CHCl_3$), IR (neat): 3311s (N–H), 2970w (C–H), 1713s (C═O), 1636m (C═C), 1539m (N–H). ^{1}H NMR (300 MHz, $CDCl_3$): δ 7.01–6.80 (m, 1H), 6.04 (br d, J = 8.5 Hz, 1H), 4.22 (q, J = 7.1 Hz, 2H), 4.10 (t, J = 4.4 Hz, 1H), 3.98–3.83 (m, 1H), 3.35 (quint, J = 5.7 Hz, 1H), 3.17–3.00 (m, 1H), 2.86 (dd, J = 18.2, 5.1 Hz, 1H), 2.13–1.95 (m, 1H), 2.06 (s, 3H), 1.64–1.46 (m, 4H), 1.42 (s, 2H), 1.30 (t, J = 7.1 Hz, 3H), 0.93 (t, J = 7.4 Hz, 3H), 0.86 (t, J = 7.4 Hz, 3H). ^{13}C NMR (75 MHz, $CDCl_3$): δ 169.7, 165.5, 134.0, 131.3, 80.3, 69.7, 60.0, 53.6, 46.3, 33.3, 25.8, 25.1, 22.7, 13.3, 8.8, 8.7.

Ethyl-(3*S*,4*R*,5*R*)-4-acetamido-5-amino-3-(pentan-3-yloxy)cyclohex-1-ene carboxylate ((3*S*,4*R*,5*R*)-1). Chlorotrimethylsilane (104.3 mg, 0.96 mmol, 0.12 mL) was added into a flask with zinc powder (815 mg, 12.5 mmol) and dry Et_2O (23 mL). The mixture was stirred for 15 min at room temperature under an inert atmosphere. Activated zinc was filtered under an inert atmosphere (Ar) and washed with dry ether (2 × 10 mL). Ethyl-(3*S*,4*R*,5*S*)-4-acetamido-5-nitro-3-(pentan-3-yloxy)cyclohex-1-ene-1-carboxylate (164 mg, 0.48 mmol) and acetic acid (9.70 g, 162 mmol, 9.3 mL) were added into the flask with activated zinc. The mixture was stirred at room temperature overnight. Zinc was filtered off, washed with EtOAc. The filtrate was concentrated under reduced pressure. The worked reaction mixture was purified by column chromatography (SiO_2, EtOAc/MeOH 2 : 1) to provide colorless powder; yield 93 mg (62%).

HRMS: m/z $[M + H]^+$ calculated: 313.213, measured: 313.212, mp = 102.8–105.5 °C, $[\alpha]_D^{20}$ = +46.7 (c = 0.5, $CHCl_3$), IR(neat): 3356w (N–H), 2964s (C–H) 1705s (C═O), 1661s (C═C), 1552s (N–H). ^{1}H NMR (600 MHz, $CDCl_3$): δ 6.86–6.83 (m, 1H), 6.06 (br d, J = 8.2 Hz, 1H), 4.32 (ddd, J = 8.3, 5.1, 2.8 Hz, 1H), 4.21 (q, J = 7.2 Hz, 2H), 4.19–4.12 (m, 1H), 3.33 (quint, J = 5.7 Hz, 1H), 3.17 (td, J = 5.6, 2.9 Hz, 1H), 2.62–2.54 (m, 1H), 2.32 (ddt, J = 18.3, 5.9, 1.7 Hz, 1H), 2.03 (s, 3H), 1.80 (br s, 2H), 1.56–1.45 (m, 4H), 1.30 (t, J = 7.1 Hz, 3H), 0.88 (dt, J = 10.5, 7.4 Hz, 6H). ^{13}C NMR (150 MHz, $CDCl_3$): δ 170.8, 166.7, 136.4, 130.0, 81.4, 70.8, 61.1, 50.6, 48.6, 33.1, 26.2, 25.9, 23.7, 14.4, 9.8, 9.4.

(3*S*,4*R*,5*S*)-4-Acetamido-5-amino-3-(pentan-3-yloxy)cyclohex-1-ene carboxylic acid ((3*S*,4*R*,5*S*)-7). 1 M water solution of NaOH (14.7 mg, 0.37 mmol) was added into a flask with aminoester (71.8 mg, 0.23 mmol) dissolved in THF (7.9 mL) at

0 °C. The reaction mixture was stirred at room temperature for 2 days. The reaction was complete after TLC detection by adding acidic amberlite (1 g). The mixture was stirred for next 15 min and subsequently amberlite was filtered off and washed with EtOH. The solvent was evaporated under reduced pressure and the worked reaction mixture was purified by flash chromatography (reverse column, acetonitrile/H_2O 19 : 1) to provide colorless powder; yield 22.0 mg (34%).

HRMS: m/z $[M + H]^+$ calculated: 285.181, measured: 285.181, mp = 174.9–179.8 °C, $[\alpha]_D^{20} = -24.8$ (c = 0.15, H_2O), IR (neat): 3357w (N–H), 2971m (C–H), 1614m (C═C), 1573s (N–H). ^{1}H NMR (600 MHz, D_2O): δ 6.67–6.43 (m, 1H), 4.29–4.27 (m, 1H), 4.24 (dd, J = 10.9, 4.6 Hz, 1H), 3.60–3.54 (m, 1H), 3.52–3.46 (m, 1H), 2.96 (dd, J = 17.6, 5.7 Hz, 1H), 2.42–2.35 (m, 1H), 2.11 (s, 3H), 1.65–1.51 (m, 4H), 0.93 (t, J = 7.5 Hz, 3H), 0.87 (t, J = 7.4 Hz, 3H). ^{13}C NMR (150 MHz, D_2O): δ 174.5, 174.1, 134.9, 130.1, 83.4, 69.9, 50.6, 46.7, 29.7, 25.4, 25.3, 22.1, 9.1, 8.3.

(3*S*,4*R*,5*R*)-4-Acetamido-5-amino-3-(pentan-3-yloxy)cyclohex-1-ene carboxylic acid ((3*S*,4*R*,5*R*)-7). 1 M water solution of NaOH (12.3 mg, 0.22 mmol) was added into a flask with the corresponding aminoester (3*S*,4*R*,5*R*)-**1** (37.5 mg, 0.12 mmol) dissolved in THF (3.7 mL) at 0 °C. The reaction mixture was stirred at room temperature overnight. The reaction was complete after TLC detection by adding acid amberlite (1 g). The mixture was stirred for next 15 min and subsequently amberlite was filtered off and washed with EtOH. The solvent was evaporated under reduced pressure and the worked reaction mixture was purified by flash chromatography (reverse column, acetonitrile/H_2O 19 : 1) to provide colorless powder; yield 8 mg (23%).

HRMS: m/z $[M + H]^+$ calculated: 285.181, measured: 285.180, mp = 178.0–181.8 °C, $[\alpha]_D^{20} = +58.9$ (c = 0.4, H_2O), IR (neat): 3331w (N–H), 2964m (C–H), 1646m (C═C), 1549s (N–H). ^{1}H NMR (600 MHz, D_2O): δ 6.43–6.40 (m, 1H), 4.82–4.76 (1H, partial covered with HOD signal), 4.66–4.61 (m, 1H), 3.71 (ddd, J = 10.8, 5.8, 2.3 Hz, 1H), 3.53–3.47 (m, 1H), 2.75 (dd, J = 17.5, 5.8 Hz, 1H), 2.39–2.30 (m, 1H), 2.09 (s, 3H), 1.68–1.40 (m, 4H), 0.90 (t, J = 7.5 Hz, 3H), 0.86 (t, J = 7.4 Hz, 3H). ^{13}C NMR (150 MHz, D_2O): δ 176.0, 173.6, 134.1, 132.0, 81.3, 71.4, 49.1, 46.8, 25.8, 25.7, 24.7, 22.0, 9.2, 8.0.

Common procedure for sample preparation for enantioselective HPLC analysis

9*H*-Fluoren-9-ylidentriphenyl-λ^5-phosphane was added into a flask with a dissolved Michael product in toluene. The reaction mixture was stirred at 100 °C for 1 h. Subsequently, the reaction mixture was cooled to room temperature and purified by column chromatography (SiO_2, hex/EtOAc) or by using a preparative TLC plate in the same mixture of solvent hex : EtOAc.

***N*-[(2*R*,3*R*)-4-[(9*Z*)-9*H*-Fluoren-9-ylidene]-1-nitro-3-(pentan-3-yloxy)butan-2-yl]acetamide and *N*-[(2*R*,3*S*)-4-[(9*Z*)-9*H*-fluoren-9-ylidene]-1-nitro-3-(pentan-3-yloxy)butan-2-yl]acetamide. According to common preparation:** *N*-[(2*R*,3*S*)-1-nitro-4-oxo-3-(pentan-3-yloxy)butan-2-yl]acetamide (104 mg, 0.36 mmol), 9*H*-fluoren-9-ylidentriphenyl-λ^5-phosphane (200 mg, 0.48 mmol), toluene (10 mL), $CHCl_3$ (1.4 mL). The reaction mixture was stirred at 100 °C for 1 h. The crude mixture was purified by column chromatography (SiO_2, hex/EtOAc 2 : 1) to provide a beige colored solid substance; yield 111 mg (68%).

(2*R*,3*R*) isomer: $[\alpha]_D^{23} = +1.9$ (c = 1.0, $CHCl_3$, dr 1 : 1 *syn*/*anti*), mp = 69.9–70.6 °C. ^{1}H NMR (300 MHz, $CDCl_3$): δ 7.79–7.60 (m, 4H), 7.44–7.27 (m, 4H), 6.42 (d, J = 9.4 Hz, 1H), 5.98 (d, J = 8.4 Hz, 1H), 5.46 (dd, J = 9.4, 4.1 Hz, 1H), 4.96–4.84 (m, 1H), 4.83–4.67 (m, 2H), 3.37 (m, 1H), 1.94 (s, 3H), 1.56–1.43 (m, 4H), 0.89 (td, J = 7.4, 1.3 Hz, 6H). ^{13}C NMR (75 MHz, $CDCl_3$): δ 169.4, 140.9, 138.6, 138.5, 137.5, 135.1, 128.3, 128.1, 126.8, 126.4, 124.3, 124.2, 119.4, 119.3, 118.8, 79.7, 73.5, 69.9, 51.2, 25.5, 24.5, 22.4, 9.1, 8.3. NOESY: without interactions between H_A (δ 5.46, dd) and H_B (δ 4.96–4.84, m). Spectral (^{1}H NMR) data corresponds with the literature.[29]

According to common preparation: *N*-[(2*R*,3*R*)-1-Nitro-4-oxo-3-(pentan-3-yloxy)butan-2-yl]acetamide (52.1 mg, 0.20 mmol), 9*H*-fluoren-9-ylidentriphenyl-λ^5-phosphane (102 mg, 0.24 mmol), toluene (5.0 mL), and $CHCl_3$ (0.8 mL). The reaction mixture was stirred at 100 °C for 1 h. The crude mixture was purified by column chromatography (SiO_2, hex/EtOAc 2 : 1) to provide a beige colored solid substance; yield 60 mg (73%).

(2*R*,3*S*) isomer: $[\alpha]_D^{23} = +38.9$ (c = 0.7, $CHCl_3$, dr 1 : 12 *syn*/*anti*), mp = 156.5–158.5 °C. ^{1}H NMR (600 MHz, $CDCl_3$): δ 8.00–7.93 (m, 1H), 7.77–7.66 (m, 3H), 7.46–7.27 (m, 4H), 6.45 (d, J = 8.7 Hz, 1H), 6.26 (d, J = 8.9 Hz, 1H), 5.38 (dd, J = 8.7, 6.0 Hz, 1H), 4.92 (dd, J = 12.8, 6.5 Hz, 1H), 4.85–4.74 (m, 1H), 4.66 (dd, J = 12.8, 3.5 Hz, 1H), 3.36–3.25 (m, 1H), 1.91 (s, 3H), 1.58–1.40 (m, 4H), 0.95–0.80 (m, 6H). ^{13}C NMR (150 MHz, $CDCl_3$): δ 170.2, 141.7, 139.8, 139.4, 138.5, 136.2, 129.2, 129.0, 128.0, 127.5, 126.4, 125.6, 120.5, 120.3, 119.8, 80.5, 74.9, 73.0, 51.7, 26.5, 25.2, 23.3, 10.1, 9.2. NOESY: Interactions between H_A (δ 5.38, dd) and H_B (δ 4.85–4.74, m).

Computation

The molecular structures of oseltamivir carboxylate stereoisomers were prepared from the crystal structure of oseltamivir bound to the viral neuraminidase of the N1 subtype (PDB entry 2HU0[30]) by inverting the hetero-substituents attached to chiral carbon atoms 3, 4 and 5. The molecular geometries of the stereoisomers were optimized by quantum chemical density functional theory (DFT)[15] with a polarizable continuum reaction field solvent model (PCM)[31] and hybrid gradient-corrected exchange–correlation functional B3LYP[32] in double-zeta Gaussian basis 6-31+G* augmented with polarization and diffuse functions[33] on all heavy atoms using the Gaussian 09 quantum chemistry software package.[34]

Electronic CD spectra of the stereoisomers were calculated by time-dependent density functional theory (TDDFT)[15] with the PCM solvent model of hydration, B3LYP functional and 6-31+G* basis set for the molecular geometries of stereoisomers optimized in water. The Cotton effects in circular dichroism spectra were generated by positioning Gaussian band-shapes over first 80 electronic transitions (rotational strengths) with a

bandwidth (FWHM) of 0.4 eV and by summing over the whole spectral range.[35]

A 3D-structure of the neuraminidase N1 : oseltamivir carboxylate complexes (influenza A virus – Viet Nam/1203/2004/H5N1) was prepared from the crystal structure obtained from the Protein Data Bank (PDB entry 2HU0[30]) by refinement and minimization using the OPLS-2005 force field.[20] Enzyme–inhibitor interactions were described by the hybrid quantum mechanical/molecular mechanical approach (QM/MM)[18a] using the QSite package of Schrödinger,[18b] where the central quantum motif (oseltamivir, side chains of 11 closest enzyme residues: Glu119, Asp151, Arg152, Ile222, Arg224, Ser246, Glu276, Glu277, Asn294, Arg371, Tyr406 and 2 structural water molecules) was described at the DFT-B3LYP/6-31+G* level. Frozen-orbital approximation was used to link covalently-bonded atoms in residues at the frontiers between the QM and MM regions.[18a] The quantum motif was embedded in a classical system comprising the remaining 376 amino acid residues of the viral neuraminidase present in the crystal structure, which were described by molecular mechanics and the OPLS-2005 force field.[20] Only a single crystal structure configuration of the neuraminidase was considered. A Poisson–Boltzmann surface area (PBSA)[36] implicit solvation model was used to include the effect of hydration on the optimized QM/MM systems.

Relative differences in enzyme–inhibitor binding energies were computed as:[19]

$$\Delta\Delta E_{\mathrm{bin,sol}} = (\Delta E_{\mathrm{tot,sol}}[\mathrm{N1:O_i}] - \Delta E_{\mathrm{tot,sol}}[\mathrm{N1}] - \Delta E_{\mathrm{tot,sol}}[\mathrm{O_i}]) - \Delta E_{\mathrm{bin,sol,Ref}}$$

for solvated optimized molecular geometries of oseltamivir carboxylate stereoisomers [O_i], enzyme : oseltamivir complexes [N1:O_i] and free enzyme [N1] using QSite[18b] at the DFT-B3LYP-PBSA/6-31+G*: OPLS-2005 level of theory. Stereoisomer I, (3*R*,4*R*,5*S*), of oseltamivir carboxylate, the active form of Tamiflu, was used as the reference structure.

Biological testing

Viruses: Human influenza A virus (IAV) A/Mississippi/1/85 (H3N2) originated from the collection of viruses of Institute of Virology, SAS, Bratislava, Slovak Republic. This virus was used as a model IAV of medium virulence.[37] To know whether the tested compounds are effective also against the Tamiflu resistant viruses, two variants of pandemic virus 2009 were included: A/Perth/265/2009 wild-type virus (H1N1 pdm09, A/California/7/2009-like) – carrying histidine at position 275 (275H) of the neuraminidase glycoprotein, Tamiflu sensitive, abbreviated as "TSV A/Perth" and A/Perth/261/2009 variant virus (H1N1 pdm09, A/California/7/2009-like) – carrying tyrosine at position 275 (275Y) of the neuraminidase glycoprotein – *i.e.* a H275Y substitution, Tamiflu resistant, abbreviated as "TRV A/Perth". These viruses were kindly provided by Aeron Hurt, the WHO Collaborating Centre for Reference and Research on Influenza, ISIRV-AVG, Melbourne, Australia. Viruses were propagated in fertilized chicken eggs and A/Perth variants were sequenced to confirm the maintenance of Tamiflu susceptibility/resistance markers. Virus stocks were aliquoted and stored at −70 °C.

Rapid culture assay (RCA): The Madin–Darby canine kidney (MDCK) cells, provided by ATCC, were cultured in Dulbecco's Modified Eagle's Medium (DMEM) supplemented with 5% fetal bovine serum on 96-microwell plates (5×10^4 cells per 100 μl per well) for 24 hours. Then, medium was removed and cell monolayers were infected with different dilutions of IAV stocks (a 100 μl per well) in Ultra-MDCK serum-free medium (Lonza) containing TPCK trypsin (2 μg mL^{-1}) and 1% DMSO. The infectious virus was detected after 18-hour incubation at 37 °C under a humid atmosphere of 5% CO_2, as described.[38] The optimal concentration of each virus strain was selected for antiviral experiments: 34 plaque forming units (pfu) per 100 μl of A/Miss virus, 8.9 pfu per 100 μl of A/Perth TRV and 11.5 pfu per 100 μl of A/Perth TSV viruses.

The antiviral efficacy of tested compounds was examined by RCA and modified as follows: Two-fold dilutions ranging in concentrations from 5000 nM to 0.078 nM of examined substances were added to MDCK cell monolayers in a volume of 50 μl per well and subsequently the virus in a predetermined optimal concentration (50 μl per well) was added. The examined compounds as well as viruses were diluted in serum-free Ultra MDCK medium containing 1% DMSO and TPCK trypsin (2 μg mL^{-1}) and were incubated at 37 °C under a humid atmosphere of 5% CO_2. After 18 hours of infection, multiple washings of cell monolayers with PBS and cell fixation with cold methanol at +4 °C for 15 minutes were done. Infectious virus was detected in cell monolayers using a monoclonal antibody (MAb) 107L (1.5 μg mL^{-1}), specific to the influenza A nucleoprotein,[39] and subsequently a second antibody, goat anti-mouse IgG conjugated with horseradish peroxidase (GAM-IgG-Px) (Bio-Rad) was added. The reaction was stopped after 1 hour incubation at 37 °C and visualized after the addition of substrate solution (100 μl per well) 3-amino-9-ethylcarbazole containing hydrogen peroxide (0.03%) as described.[38] After 30 min incubation/25 °C, the plates were washed with PBS and the results were evaluated microscopically. Differentially red stained cells were considered as positive for infection. The percentage of inhibition of red color staining in comparison to the controls without any antiviral compound was evaluated.

Monoclonal antibody preparation: Influenza A nucleoprotein-specific MAb 107L was prepared at the Institute of Virology, Slovak Republic as described before.[39]

Acknowledgements

This work was supported by the Slovak Research and Development Agency under the contract no. APVV-0067-11, and by the Scientific Grant Agency of Ministry of Education of Slovak Republic and Slovak Academy of Sciences under grants VEGA no. 2/0146/15, no. 2/0100/13, and 2/0106/17. We thank

Dr. Juraj Filo (Comenius University in Bratislava) for NMR analyses.

Notes and references

1 WHO, *Influenza (Seasonal), Fact sheet No. 211*, 2014.
2 WHO, *Model List of Essential Medicines*, 19th list edn, 2015, p. http://www.who.int/medicines/publications/essential-medicines/en/index.html.
3 M. von Itzstein, *Nat. Rev. Drug Discovery*, 2007, **6**, 967–974.
4 M. Federspiel, R. Fischer, M. Hennig, H.-J. Mair, T. Oberhauser, G. Rimmler, T. Albiez, J. Bruhin, H. Estermann, C. Gandert, V. Göckel, S. Götzö, U. Hoffmann, G. Huber, G. Janatsch, S. Lauper, O. Röckel-Stäbler, R. Trussardi and A. G. Zwahlen, *Org. Process Res. Dev.*, 1999, **3**, 266–274.
5 (*a*) J. Magano, *Chem. Rev.*, 2009, **109**, 4398–4438; (*b*) M. Shibasaki, M. Kanai and K. Yamatsugu, *Isr. J. Chem.*, 2011, **51**, 316–328; (*c*) J. Magano, *Tetrahedron*, 2011, **67**, 7875–7899; (*d*) M. Shibasaki and M. Kanai, *Eur. J. Org. Chem.*, 2008, 1839–1850.
6 D. Enders, M. R. M. Huttl, C. Grondal and G. Raabe, *Nature*, 2006, **441**, 861–863.
7 (*a*) H. Ishikawa, T. Suzuki and Y. Hayashi, *Angew. Chem., Int. Ed.*, 2009, **48**, 1304–1307; (*b*) H. Ishikawa, T. Suzuki, H. Orita, T. Uchimaru and Y. Hayashi, *Chem. – Eur. J.*, 2010, **16**, 12616–12626.
8 (*a*) S. Zhu, S. Yu, Y. Wang and D. Ma, *Angew. Chem., Int. Ed.*, 2010, **49**, 4656–4660; (*b*) J. Rehák, M. Huťka, A. Latika, H. Brath, A. Almássy, V. Hajzer, J. Durmis, S. Toma and R. Šebesta, *Synthesis*, 2012, 2424–2430; (*c*) J. Weng, Y.-B. Li, R.-B. Wang and G. Lu, *ChemCatChem*, 2012, **4**, 1007–1012.
9 (*a*) T. Mukaiyama, H. Ishikawa, H. Koshino and Y. Hayashi, *Chem. – Eur. J.*, 2013, **19**, 17789–17800; (*b*) Y. Hayashi and S. Ogasawara, *Org. Lett.*, 2016, **18**, 3426–3429.
10 P. Tisovský, T. Peňaška, M. Mečiarová and R. Šebesta, *ACS Sustainable Chem. Eng.*, 2015, **3**, 3429–3434.
11 (*a*) C. Suttibut, Y. Kohari, K. Igarashi, H. Nakano, M. Hirama, C. Seki, H. Matsuyama, K. Uwai, N. Takano, Y. Okuyama, K. Osone, M. Takeshita and E. Kwon, *Tetrahedron Lett.*, 2011, **52**, 4745–4748; (*b*) H. Nakano, K. Osone, M. Takeshita, E. Kwon, C. Seki, H. Matsuyama, N. Takano and Y. Kohari, *Chem. Commun.*, 2010, **46**, 4827–4829.
12 A. Sartori, L. Dell'Amico, L. Battistini, C. Curti, S. Rivara, D. Pala, P. S. Kerry, G. Pelosi, G. Casiraghi, G. Rassu and F. Zanardi, *Org. Biomol. Chem.*, 2014, **12**, 1561–1569.
13 A. Krówczyński and L. Kozerski, *Synthesis*, 1983, 489–491.
14 J. W. Johnson, D. P. Evanoff, M. E. Savard, G. Lange, T. R. Ramadhar, A. Assoud, N. J. Taylor and G. I. Dmitrienko, *J. Org. Chem.*, 2008, **73**, 6970–6982.
15 (*a*) J. Autschbach, L. Nitsch-Velasquez and M. Rudolph, in *Electronic and Magnetic Properties of Chiral Molecules and Supramolecular Architectures*, ed. R. Naaman, N. D. Beratan and D. Waldeck, Springer Berlin Heidelberg, Berlin, Heidelberg, 2011, pp. 1–98; (*b*) F. Furche and D. Rappoport, in *Computational Photochemistry*, ed. M. Olivucci, Elsevier Science, Amsterdam, 2005.
16 G. Pescitelli and T. Bruhn, *Chirality*, 2016, **28**, 466–474.
17 M. Gorecki, *Org. Biomol. Chem.*, 2015, **13**, 2999–3010.
18 (*a*) R. A. Friesner and V. Guallar, *Annu. Rev. Phys. Chem.*, 2005, **56**, 389–427; (*b*) *Small-Molecule Drug Discovery Suite 2014-2*, Schrödinger, LLC, New York, QSite version 6.3 edn, 2014.
19 (*a*) V. Frecer, S. Miertuš, A. Tossi and D. Romeo, *Drug Des. Discovery*, 1998, **15**, 211–231; (*b*) V. Frecer, F. Berti, F. Benedetti and S. Miertus, *J. Mol. Graphics Modell.*, 2008, **27**, 376–387; (*c*) V. Frecer, E. Megnassan and S. Miertus, *Eur. J. Med. Chem.*, 2009, **44**, 3009–3019.
20 J. L. Banks, H. S. Beard, Y. Cao, A. E. Cho, W. Damm, R. Farid, A. K. Felts, T. A. Halgren, D. T. Mainz, J. R. Maple, R. Murphy, D. M. Philipp, M. P. Repasky, L. Y. Zhang, B. J. Berne, R. A. Friesner, E. Gallicchio and R. M. Levy, *J. Comput. Chem.*, 2005, **26**, 1752–1780.
21 T. Rungrotmongkol, V. Frecer, W. De-Eknamkul, S. Hannongbua and S. Miertus, *Antiviral Res.*, 2009, **82**, 51–58.
22 W. L. F. Armarego and C. L. L. Chai, *Purification of Laboratory Chemicals*, Elsevier, 6th edn, Online version available at http://www.knovel.com, 2009.
23 M. Faulques, L. Rene and R. Royer, *Synthesis*, 1982, 260–261.
24 A. Kamimura and N. Ono, *Synthesis*, 1988, 921–922.
25 J. Weng, Y.-B. Li, R.-B. Wang, F.-Q. Li, C. Liu, A. S. C. Chan and G. Lu, *J. Org. Chem.*, 2010, **75**, 3125–3128.
26 T. Arai, F. Konno, M. Ogawa, M.-R. Zhang and K. Suzuki, *J. Labelled Compd. Radiopharm.*, 2009, **52**, 350–354.
27 R. B. Parthasaradhi, R. K. Rathnakar, R. R. Raji, R. D. Muralidhara and C. R. K. Subash, *Process for obtaining pure oseltamivir*, WO077570A1, 2007.
28 J.-J. Shie, J.-M. Fang, S.-Y. Wang, K.-C. Tsai, Y.-S. E. Cheng, A.-S. Yang, S.-C. Hsiao, C.-Y. Su and C.-H. Wong, *J. Am. Chem. Soc.*, 2007, **129**, 11892–11893.
29 V. Hajzer, A. Latika, J. Durmis and R. Šebesta, *Helv. Chim. Acta*, 2012, **95**, 2421–2428.
30 R. J. Russell, L. F. Haire, D. J. Stevens, P. J. Collins, Y. P. Lin, G. M. Blackburn, A. J. Hay, S. J. Gamblin and J. J. Skehel, *Nature*, 2006, **443**, 45–49.
31 (*a*) S. Miertuš, E. Scrocco and J. Tomasi, *Chem. Phys.*, 1981, **55**, 117–129; (*b*) S. Miertuš and J. Tomasi, *Chem. Phys.*, 1982, **65**, 239–245.
32 A. D. Becke, *J. Chem. Phys.*, 1993, **98**, 5648–5652.
33 (*a*) R. Krishnan, J. S. Binkley, R. Seeger and J. A. Pople, *J. Chem. Phys.*, 1980, **72**, 650–654; (*b*) A. D. McLean and G. S. Chandler, *J. Chem. Phys.*, 1980, **72**, 5639–5648.
34 M. J. T. Frisch, G. W. Trucks, H. B. Schlegel, G. E. Scuseria, M. A. Robb, J. R. Cheeseman, G. Scalmani, V. Barone, B. Mennucci, G. A. Petersson, H. Nakatsuji, M. Caricato, X. Li, H. P. Hratchian, A. F. Izmaylov, J. Bloino, G. Zheng, J. L. Sonnenberg, M. Hada, M. Ehara, K. Toyota, R. Fukuda, J. Hasegawa, M. Ishida, T. Nakajima, Y. Honda, O. Kitao,

H. Nakai, T. Vreven, J. A. Montgomery Jr., J. E. Peralta, F. Ogliaro, M. Bearpark, J. J. Heyd, E. Brothers, K. N. Kudin, V. N. Staroverov, R. Kobayashi, J. Normand, K. Raghavachari, A. Rendell, J. C. Burant, S. S. Iyengar, J. Tomasi, M. Cossi, N. Rega, J. M. Millam, M. Klene, J. E. Knox, J. B. Cross, V. Bakken, C. Adamo, J. Jaramillo, R. Gomperts, R. E. Stratmann, O. Yazyev, A. J. Austin, R. Cammi, C. Pomelli, J. W. Ochterski, R. L. Martin, K. Morokuma, V. G. Zakrzewski, G. A. Voth, P. Salvador, J. J. Dannenberg, S. Dapprich, A. D. Daniels, Ö. Farkas, J. B. Foresman, J. V. Ortiz, J. Cioslowski and D. J. Fox, *Gaussian 09, Revision E.01*, Gaussian, Inc., Wallingford CT, USA, 2009.

35 (*a*) P. J. Stephens, F. J. Devlin, C. F. Chabalowski and M. J. Frisch, *J. Phys. Chem.*, 1994, **98**, 11623–11627; (*b*) P. J. Stephens and N. Harada, *Chirality*, 2010, **22**, 229–233.

36 Q. Cai, M.-J. Hsieh, J. Wang and R. Luo, *J. Chem. Theor. Comput.*, 2010, **6**, 203–211.

37 T. Fislová, M. Gocník, T. Sládková, V. Ďurmanová, J. Rajčáni, E. Varečková, V. Mucha and F. Kostolanský, *Arch. Virol.*, 2009, **154**, 409–419.

38 E. Varečková, N. Cox and A. Klimov, *J. Clin. Microbiol.*, 2002, **40**, 2220–2223.

39 E. Varečková, T. Betáková, V. Mucha, L. Soláriková, F. Kostolanský, M. Waris and G. Russ, *J. Immunol. Methods*, 1995, **180**, 107–116.